Supplementary Information for

Damp-heat stable and efficient perovskite solar cells and mini-modules with *t*BP-free hole-transporting layer

Yun Seop Shin,‡[ab] *Jaehwi Lee*,‡[b] *Dong Gyu Lee*,‡[c] *Ji Won Song*,[a] *Jongdeuk Seo*,[b] *Jina Roe*,[b] *Min Jung Sung*,[a] *Sujung Park*,[d] *Gwang Yong Shin*,[c] *Jiwoo Yeop*,[b] *Dongmin Lee*,[a] *Chang Hyeon Yoon*,[a] *Minseong Kim*,[a] *Jung Geon Son*,[b] *Gi-Hwan Kim*,[c] *Shinuk Cho*,[d] *Jin Young Kim*,[ab] *Tae Kyung Lee*,[ce]* and *Dong Suk Kim*[ab]*

[a]Graduate School of Carbon Neutrality, Ulsan National Institute of Science and Technology (UNIST), Ulsan 44919, Republic of Korea

[b]School of Energy and Chemical Engineering, Ulsan National Institute of Science and Technology (UNIST), Ulsan 44919, Republic of Korea

[c]Department of Materials Engineering and Convergence Technology, Gyeongsang National University (GNU), Jinju 52828, Republic of Korea

[d]Department of Physics and Energy Harvest Storage Research Center, University of Ulsan, Ulsan 44610, Republic of Korea

[e]School of Materials Science and Engineering, Gyeongsang National University (GNU), Jinju 52828, Republic of Korea

‡These authors equally contributed to this work

*Corresponding author. E-mail: tklee8865@gnu.ac.kr; kimds@unist.ac.kr

Experimental Section

Materials

Fluorine-doped tin oxide on glass (FTO) was purchased from Asahi. Hydrogen peroxide (H_2O_2, electronic grade), ethanol (EtOH, 95%, special grade), and ethyl ether (99.5%, special grade) were purchased from SAMCHUN. Hydrochloride (HCl, 37 wt% in water) was purchased from Junsei Chemical Co. Methylammonium chloride (MACl, for synthesis), *N*,*N*-dimethylformamide (DMF, anhydrous 99.8%), dimethyl sulfoxide (DMSO, >99.5%), 2-propanol (IPA, anhydrous, 99.5%), 2-methoxyethanol (2-ME, anhydrous, 99.8%), acetonitrile (anhydrous, 99.8%), chlorobenzene (CB, anhydrous, 99.8%), titanium diisopropoxide bis(acetylacetonate) ($Ti(acac)_2$, 75 wt% in IPA), potassium chloride (KCl, ACS reagent, 99.999% trace metals basis), urea (ACS reagent, 99.0-100.5%), thioglycolic acid (TGA, ≥99%), tin(II) chloride dihydrate ($SnCl_2 \cdot 2H_2O$, ≥99.995%), lithium bis(trifluoromethanesulfonyl)imide salt (LiTFSI), 4-*tert*-Butylpyridine (*t*BP, 98%), and ethylene carbonate (EC, 98%) were purchased from Sigma-Aldrich. Tin (IV) oxide (SnO_2, 12% in H_2O colloidal dispersion) was purchased from Xi'an Yuri Solar Co. Lead(II) iodide (PbI_2, 99.99% trace metal basis) was purchased from TCI. Formamidinium iodide (FAI) and *n*-octylammonium iodide (OAI) was purchased from Greatcell Solar Materials. Spiro-OMeTAD (99.5%) and FK209 Co(III) TFSI salt (>99%) were purchased from Lumtec.

Material synthesis

Formamidinium lead triiodide ($FAPbI_3$) black powder was synthesized by mixing FAI (0.8M concentration) with PbI_2 (1:1 molar ratio) in 2-ME under stirring. The mixture was gradually heated to 120 ℃ while stirring, and the precipitated $FAPbI_3$ powder was washed three times with ether. After filtration using a glass filter, the black powder was baked at 150 ℃ for 30 minutes.

PSCs substrate preparation

FTO glass was cleaned following the RCA-SC2 procedure using blends of H_2O_2, HCl, and H_2O, and subsequently, acetone and IPA were used sequentially in an ultrasonic bath. The chemical bath deposition (CBD) solution was prepared by mixing 625 mg of urea, 625 mL of HCl, 12.5 mL of TGA, and 137.5 mg of $SnCl_2 \cdot 2H_2O$ in 300 mL of DI water. After one edge of the FTO substate was taped with kapton tape to mitigate the deposition of SnO_2, these substrates, along with the CBD solution, were loaded onto a Hellendahl staining glass bath. This reaction bath was stored in an oven at 70 ℃ for 4−6 hours to reach the target pH, after which further cleaning with DI water and IPA was performed sequentially. Lastly, the substrates

were annealed at 170 °C for 60 minutes under ambient condition to dry the residual solvent, followed by treating 3 mg/mL KCl in DI water at 3,000 rpm for 30 seconds and annealing at 100 °C for 30 minutes.

PSCs fabrication

The whole process of the PSCs fabrication was carried out at controlled dry room (20 °C/20% RH). The perovskite precursor solution was prepared by mixing 1,202 mg $FAPbI_3$, 35 mol% MACl, and 0.8 mol% $MAPbBr_3$ in a mixture of DMF and DMSO (4:1). The filtered perovskite solution, using a 0.2 μm PVDF filter, was spread over the as-prepared SnO_2 substrate at 7,500 rpm for 50 seconds with a ramping duration of 0.1 seconds. During the spin-coating process, 1 mL of diethyl ether, serving as an anti-solvent, was dripped after spinning for 13 seconds, followed by immediate annealing on a hot plate at 150 °C for 15 minutes. To passivate the surface of the perovskite, 4 mg/mL of octylammonium iodide dissolved in IPA was spin-coated on top of the perovskite film at 3,000 rpm for 30 seconds. After then, the hole-transporting layer was deposited by spin-coating a spiro-OMeTAD (Lumtech) solution, containing 3 μL of LiTFSI, at 4,000 rpm for 30 seconds. For the target conditions, an EC-incorporated CB solvent at a concentration of 5 mM was utilized to dissolve spiro-OMeTAD. Finally, a gold electrode (80 nm) was deposited by thermal evaporation under a high vacuum of 10^{-6} Torr.

PSMs fabrication

For the P1 process, 5 × 5 cm^2 and 10 × 10 cm^2 FTO substrates were scribed using a picosecond laser (Advanced Optowave, AMT 532) with a scribing width of 25 μm. The substrates were scribed with 10 and 18 strips connected in series at a laser power of 2 W, a speed of 200 mm s^{-1}, and a frequency of 500 kHz. In the following steps for the ETL, a compact TiO_2 (c-TiO_2) solution was prepared by diluting $Ti(acac)_2$ in EtOH (1:15 v/v %). The TiO_2 solution was then sprayed onto the scribed FTO substrates at 450 °C, and the substrates were subsequently annealed at 450 °C for 1 hour. Next, the diluted SnO_2 nanoparticles were dropped onto the c-TiO_2 substrates, and then stored in a vacuum oven at 100 °C for 1 hour. For the perovskite layer deposition, 1,139 mg $FAPbI_3$, 42.54 mg MACl, 74.68 mg PbI_2 and 17.24 mg $MAPbBr_3$ were dissolved in 1 mL DMF/DMSO (4:1 v/v %). The perovskite solution was filtered through a 0.2 μm PVDF filter and coated onto the as-prepared ETL substrate at 5,000 rpm for 50 seconds with a ramping duration of 0.1 second. During the spin-coating process, 5 mL of diethyl ether, used as an anti-solvent, was dropped after 15 seconds of spinning. This was immediately followed by sequential annealing on a hot plate at 150 °C for 15 minutes and then 100 °C for 1 hour. The passivation and HTL fabrication were conducted in the same manner as for the small-sized PSCs. The P2 lines (90 μm width) were patterned with a laser power of 0.6 W, a speed of 200 mm s^{-1}, and a frequency of 500 kHz. The distance between the P1 and P2 lines was approximately 75 μm. Finally, the Au top electrode was deposited with a thickness of 80 nm.

The P3 process (42 μm width) was scribed with a laser power of 0.6 W, a speed of 200 nm s^{-1}, and a frequency of 500 kHz. The distance between the P2 and P3 was approximately 56 μm.

Characterization of the spiro-OMeTAD and perovskite films

FT-IR spectra were measured using a spectrometer with attenuated total reflection mode (670-IR, Varian). UV-visible absorption spectra were measured using a spectrophotometer (Cary 5000, Agilent). ESR spectra were measured using a spectrometer (EMXplus, Bruker Optics). AFM images were obtained with a microscope (Dimension ICON, Bruker Nano Surface). Surface potential was measured using a Kelvin probe force microscope (Nanocute, SII NanoTechnology Inc.). The potential was measured using two independent lock-in amplifiers, with the cantilever resonance frequency serving as the feedback. The probe used was a Rh-coated Si cantilever with a resonance frequency of 25 kHz. UPS spectra were measured using a spectrometer (ESCALAB 250XI, Thermo Fisher Scientific) at a base pressure of 1.0×10^{-9} Torr with a monochromated Al-Kα X-ray source. XRD patterns of the perovskite films were measured using a diffractometer (D8 ADVANCE, Bruker AXS) equipped with Cu-Kα radiation, ($\lambda = 0.1542$ nm) as the X-ray source.

NMR measurements

Solution ^{1}H and ^{7}Li spectra were measured using a 400 MHz FT-NMR spectrometer (AVANCE III HD, Bruker Optics) equipped with a 5 mm BBO probe. A zg30 pulse sequence was used with a 90° pulse width. For ^{1}H spectra, a recycle delay of 1 second was used, with an acquisition time of 4.0894 seconds at a resonance frequency of 400.22 MHz. For ^{7}Li spectra, a recycle delay of 5 seconds was used, with an acquisition time of 3.5127 seconds at a resonance frequency of 155.54 MHz. The total number of scans was 16. ^{7}Li-^{1}H HOESY spectra were measured using a 600 MHz FT-NMR spectrometer (ADVANCE NEO 600, Bruker Optics) equipped with a 5 mm Prodigy probe and a hoesyetgp pulse sequence. A recycle delay of 3.57 seconds was used, with a mixing time of 1.83 seconds. The number of scans were 4, with 16 dummy scans.

ToF-SIMS measurements

ToF-SIMS profiling measured the depth distribution of ions within the structure of FTO/SnO_2/perovskite/spiro-OMeTAD/Au after light illumination and thermal stress using a spectrometer (ToF-SIMS 5, ION TOF) equipped with a pulsed Bi^{+} cluster ion beam (25 keV and 1 pA). To accomplish the depth profiling measurement, Cs (0.25 keV and 12 nA) and O_2 (0.5 keV, 88 nA) ion beams were utilized for negative and positive modes, respectively. The sputter size was 250 × 250 μm, while the analysis area for depth profiling was 50 × 50 μm.

DMA measurements

Glass transition temperature of spiro-OMeTAD was measured using a thermal analyzer (DMA Q850, TA Instruments) in stretch mode, with a maximum displacement amplitude of 15 μm, a vibration frequency of 1 Hz, and a heating rate of 3 °C/min from 30 to 150 °C. Samples were prepared using poly(propylene) (PP).

Characterization of PSCs and PSMs

Unencapsulated PSCs were measured with a solar simulator (Newport-Oriel 94083A, Class AAA) in conjunction with a Keithley source meter 2400, under ambient conditions (25 °C/20% RH). The light intensity was calibrated to AM 1.5G (100 mW/cm^2) using a Si-reference cell certified by the National Renewable Energy Laboratory. The conventional *J-V* curves were measured under both forward (from a forward bias (−0.05 V) to a short circuit (1.25 V)) and reverse (from a forward bias (1.25 V) to a short circuit (−0.05 V)) scans with the fixed step voltage of 100 mV. For PSMs with aperture areas of 25 and 100 cm^2, the voltage ranges were fixed at 13 V to −0.1 V and 21 V to −0.1 V under reverse bias, respectively. To mitigate artifacts induced by scattered light, a non-reflective mask with an aperture area of 0.0803 cm^2 was used to shield the active area of the device. EQEs were measured using a quantum efficiency measurement system (QUANTX-300, Newport Co.).

Characterization of PSCs and PSMs stability

The damp-heat (85 °C/85% RH) stability test was conducted using a temperature & humidity chamber (TH3-PE, Jeio Tech Co. Ltd). The performance of the devices was periodically assessed following their cooling to room temperature. The operational stability test was conducted using a white LED calibrated to AM 1.5G (100 mW/cm^2), with the PSCs housed in a home-built sample holder purged with a continuous flow of N_2. *J-V* curves with reverse scans were recorded every hour during the operational test.

Computational details

A. Density functional theory (DFT) calculation

All DFT calculations were performed using DMol^3 program[S1,S2] to investigate the electrostatic potential (ESP) charges, ESP isosurfaces, binding energies, and binding Gibbs free energies. Becke's three-parameter hybrid exchange functional with the Lee–Yang–Parr correlation functional was used to describe the exchange-correlation energy.[S3,S4] The van der Waals interactions was corrected using Tkatchenko-Scheffler method.[S5] Spin-polarized calculations

were employed, and orbital cut-off distance was set at 5.1 Å. For the geometry optimization, the convergence criteria of energy, force, displacement, and self-consistent field were set to 1 × 10^{-5} Ha, 0.002 Ha/Å, 0.005 Å, and 1 × 10^{-6} Ha, respectively. All electron relativistic core treatments and double numerical plus polarization (version 4.4) basis set were adopted to describe the core electrons and the atomic orbital basis set, respectively.

The binding energies of Li^+ ion with $(EC)_n$ were calculated by following equation.

$$\text{Binding energy} = \frac{E_{Li^+\text{-}(EC)_n} - E_{Li^+} - n \times E_{EC}}{n_{EC}} \qquad \textbf{(Equation S1)}$$

where $E_{Li^+\text{-}(EC)_n}$, E_{Li^+}, E_{EC}, n, and n_{EC} are the total energy of Li^+ ion in complex with $(EC)_n$, the energy of the Li^+ ion, the energy of EC molecule, the number of molecules, and the number of EC molecules, respectively.

The binding energies of the Li^+ ion with $TFSI^-$ anion were calculated by the following equation.

$$\text{Binding energy} = E_{total} - E_{Li^+} - E_{TFSI^-} \qquad \textbf{(Equation S2)}$$

where E_{total}, E_{Li^+}, and E_{TFSI^-} are the total energy of Li^+ ion with $TFSI^-$ anion, the energy of Li^+ ion, and the energy of $TFSI^-$ anion, respectively.

The binding energy of the spiro-OMeTAD$^{\bullet+}$ with $TFSI^-$ anion was calculated by the following equation.

$$\text{Binding energy} = E_{total} - E_{\text{spiro-OMeTAD}^{\bullet+}} - E_{TFSI^-} \qquad \textbf{(Equation S3)}$$

where E_{total}, $E_{\text{spiro-OMeTAD}^{\bullet+}}$, and E_{TFSI^-} are the total energy of spiro-OMeTAD$^{\bullet+}$ with $TFSI^-$ anion, the energy of spiro-OMeTAD$^{\bullet+}$, and the energy of $TFSI^-$ anion, respectively.

The binding Gibbs free energies (ΔG) of the Li^+ ion with $(EC)_n$ were calculated by the following equation.

$$\Delta G = \frac{G_{Li^+\text{-}(EC)_n} - G_{Li^+} - n \times G_{EC}}{n_{EC}} \qquad \textbf{(Equation S4)}$$

where $G_{Li^+\text{-}(EC)_n}$, G_{Li^+}, G_{EC}, n, and n_{EC} are the total energy of Li^+ ion in complex with $(EC)_n$, the energy of the Li^+ ion, the energy of EC molecule, the number of molecules, and the number of EC molecules, respectively.

For the modeling of initial configurations of the Li^+ ion with $(EC)_n$, Monte Carlo (MC) simulations were performed by using Sorption program. The COMPASS III forcefield[S6] was used in the MC simulations. The maximum loading and the production steps were 1 × 10^5. The atom-based summation method with a cut-off distance of 12.5 Å was considered for van der Waals interactions and the Ewald method with a 0.001 kcal/mol accuracy was used for electrostatic interactions.

B. Molecular dynamics (MD) simulation

MD simulations were employed to investigate the effect of EC molecules on Li^+ ion solvation characteristics. We used the atomic charge of each molecule by obtaining ESP charges from the DFT calculations. Moreover, atomic charges of Li^+ ion and $TFSI^-$ anions were scaled using the refractive index of EC (*i.e.*, 1.42) based on previous studies;[S7,S8] the scaling factor is 0.704. All MD simulations were performed with the COMPASS III forcefield.[S6] Atom-based summation method with a cut-off distance of 12.5 Å was considered for van der Waals interactions and particle-particle particle-mesh method with a 0.001 kcal/mol accuracy was used for electrostatic interactions. The *NPT* ensemble (isothermal-isobaric ensemble, $P = 1$ atm, $T = 25$ °C or 85 °C) was simulated for 5 ns using Berendsen thermostat and barostat[S9] using a 1 fs time step. After the *NPT* simulations, the *NVT* ensemble (canonical ensemble) was simulated for 40 ns using Berendsen thermostat using a 1 fs time step. After the *NVT* simulations, the analyses of MD simulations were performed from the 38.5 ns to 40 ns.

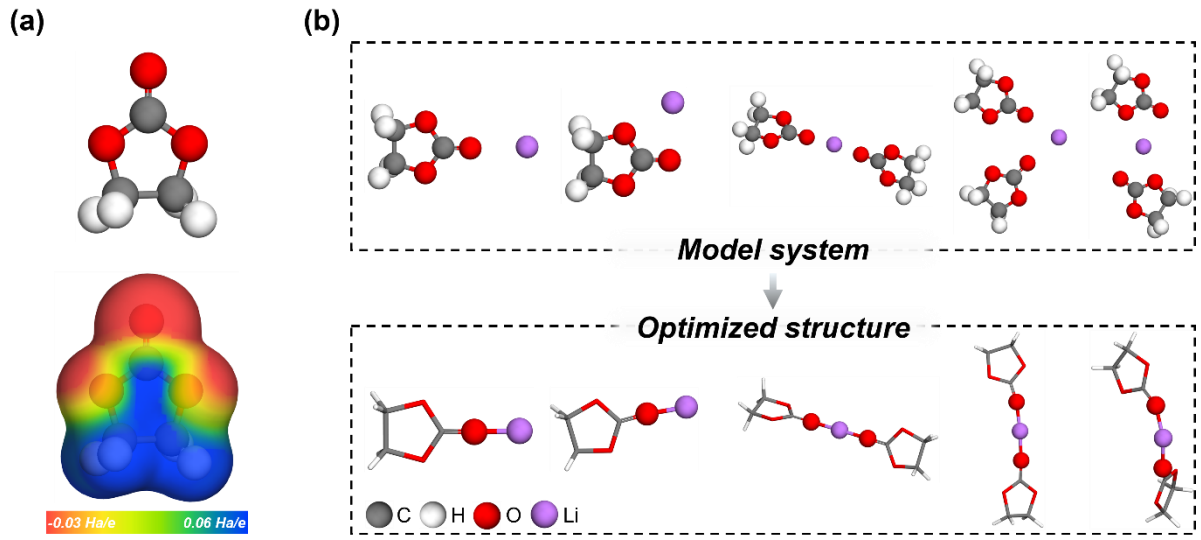

Fig. S1 (a) Electrostatic potential isosurface of ethylene carbonate (EC). The isovalue is 0.03 *e*/Å. (b) Model systems and optimized structures for investigating the binding sites of Li^+ ions in the EC molecule.

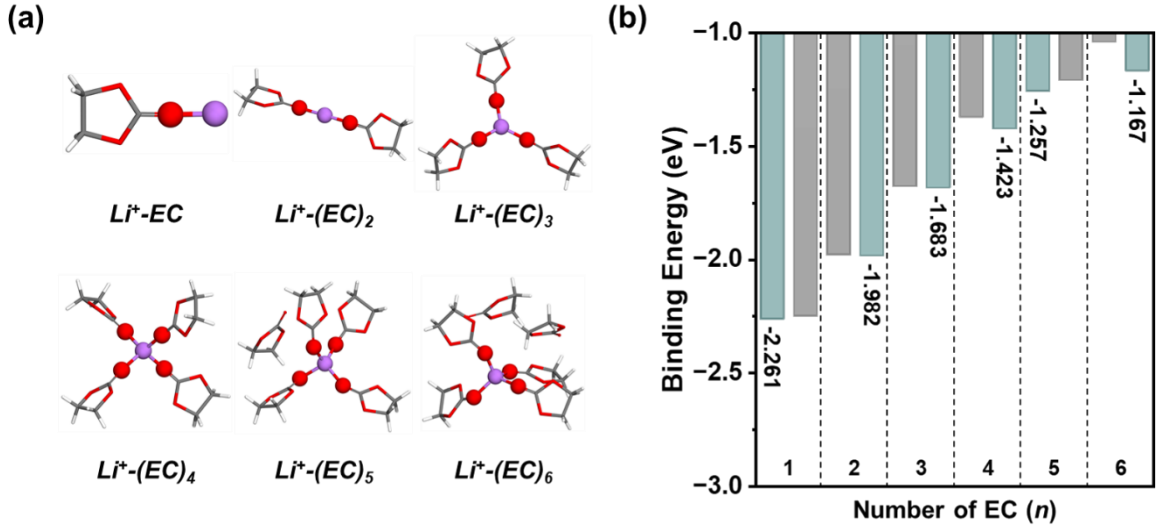

Fig. S2 (a) Most thermodynamically stable configurations of Li^+ ion with $(EC)_n$. (b) Binding energies of Li^+ ion with $(EC)_n$, where *n* denotes the number of EC molecules. The mint blue colored bars represent the most thermodynamically stable binding energy in each system.

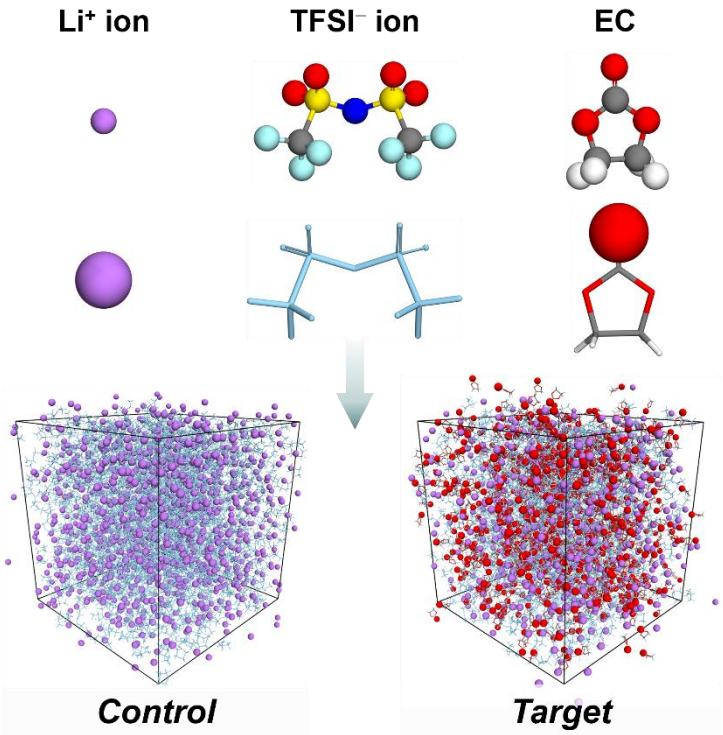

Fig. S3 Model systems for molecular dynamics simulations based on experimental conditions (*i.e.*, control and target conditions).

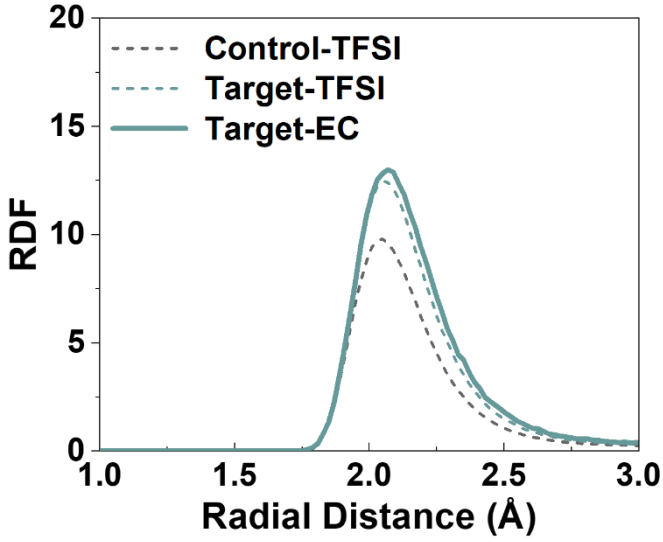

Fig. S4 Radial distribution function (RDF) of the Li^+ ion with the $TFSI^-$ ion (oxygen atom) and EC (oxygen atom in the C=O bond) under control and target conditions at 25 °C.

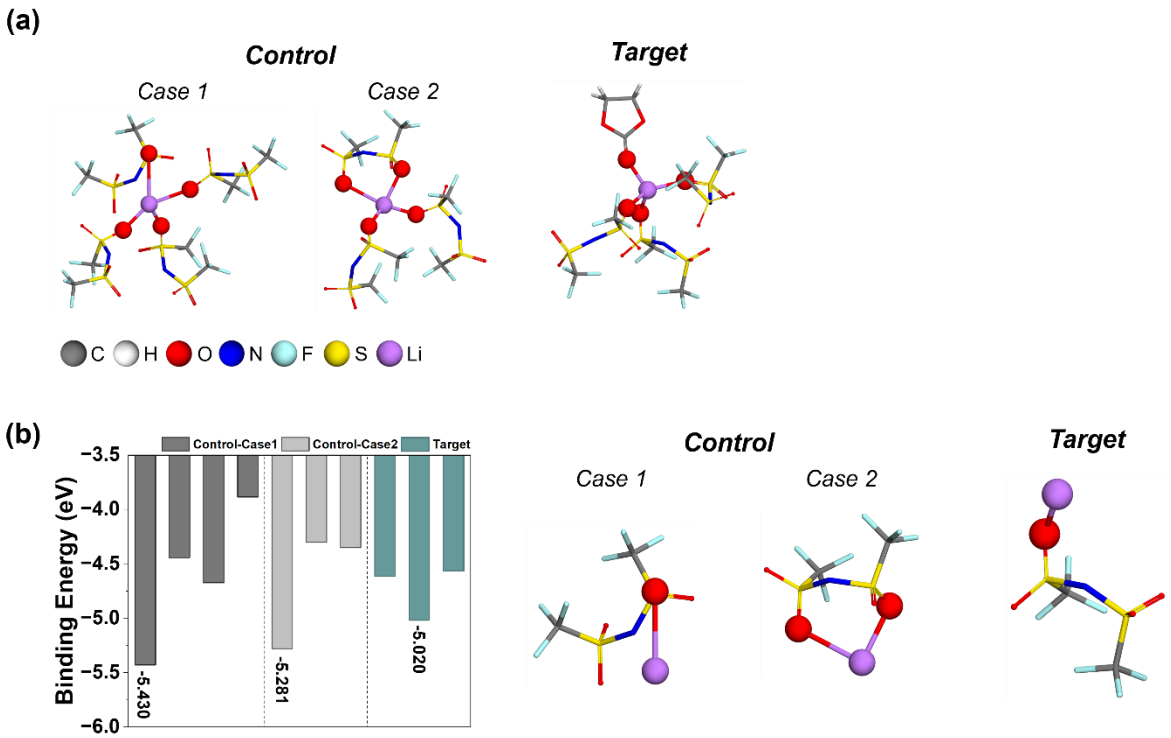

Fig. S5 (a) The complex structures of the Li^+ ion with the $TFSI^-$ ion and EC molecule, obtained from molecular dynamics simulations under control and target conditions at 25 °C. (b) Binding energies of the Li^+ ion with the $TFSI^-$ ion in the complex structures shown in (a), and the most thermodynamically stable configuration under each condition at 25 °C. The binding energies were obtained through single-point energy calculations.

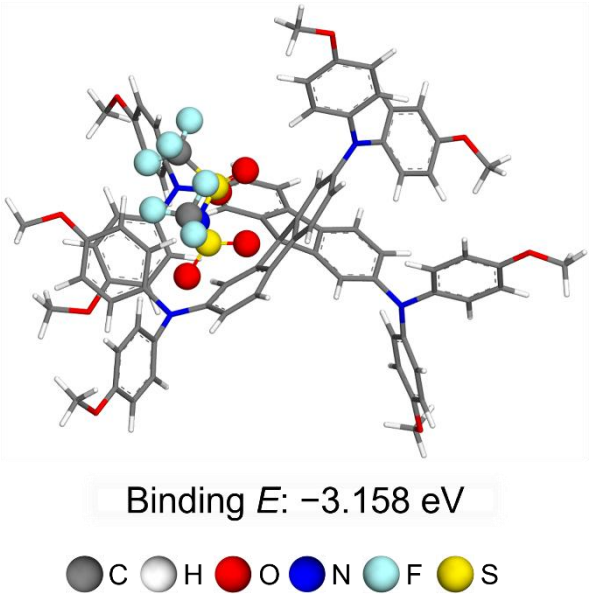

Fig. S6 Geometrically optimized structure and binding energy of spiro-OMeTAD$^{\bullet+}$ with TFSI^{-} ion.

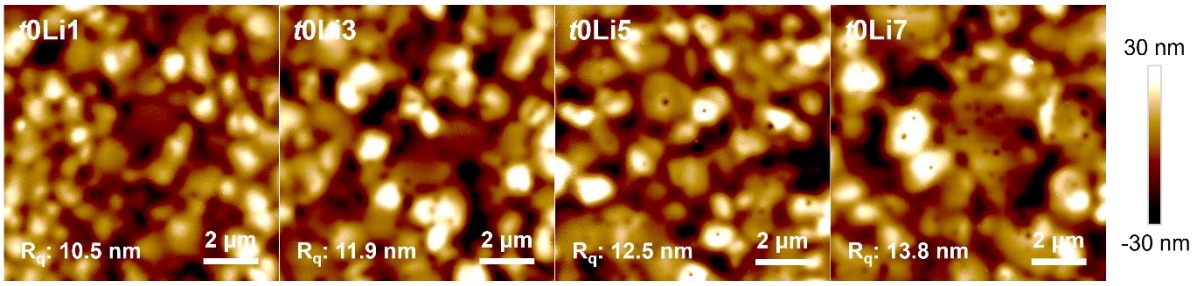

Fig. S7 AFM images of as-prepared spiro-OMeTAD films deposited onto the perovskite layer for various LiTFSI dopant concentrations while maintaining a fixed *t*BP content of 0 µL. The scale bar is 2 µm.

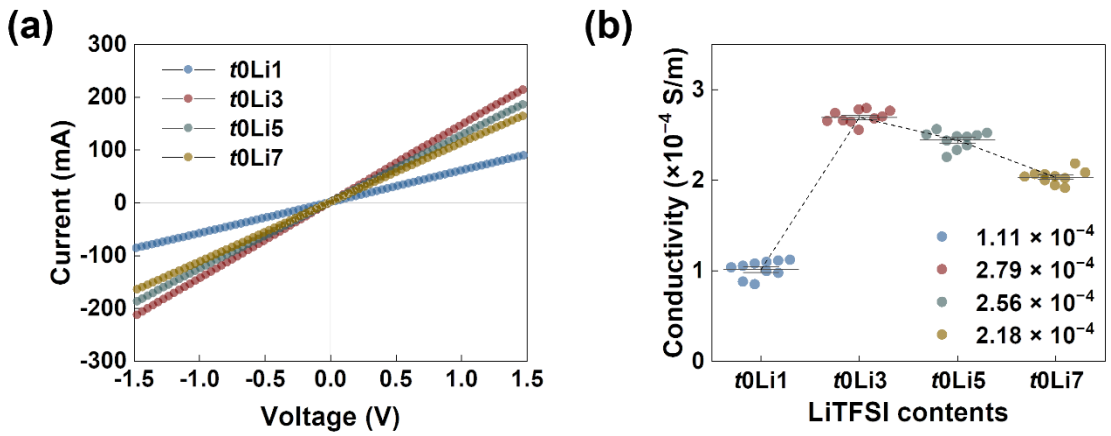

Fig. S8 (a) *J-V* curves measured with the FTO/spiro-OMeTAD/Au hole only device for evaluating the conductivity of spiro-OMeTAD films. (b) Electrical conductivities of spiro-OMeTAD films as a function of the LiTFSI dopant concentration for a fixed *t*BP content of 0 μL.

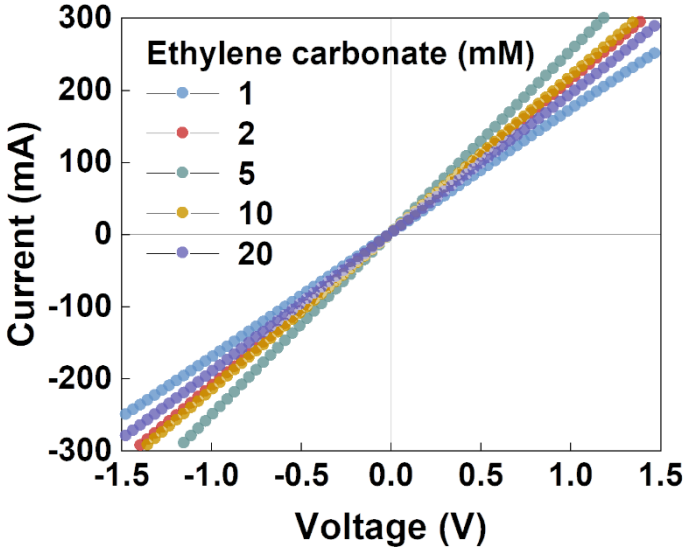

Fig. S9 *J-V* curves measured with the FTO/spiro-OMeTAD/Au hole only device for evaluating the conductivity of spiro-OMeTAD films under different concentrations of the EC additive.

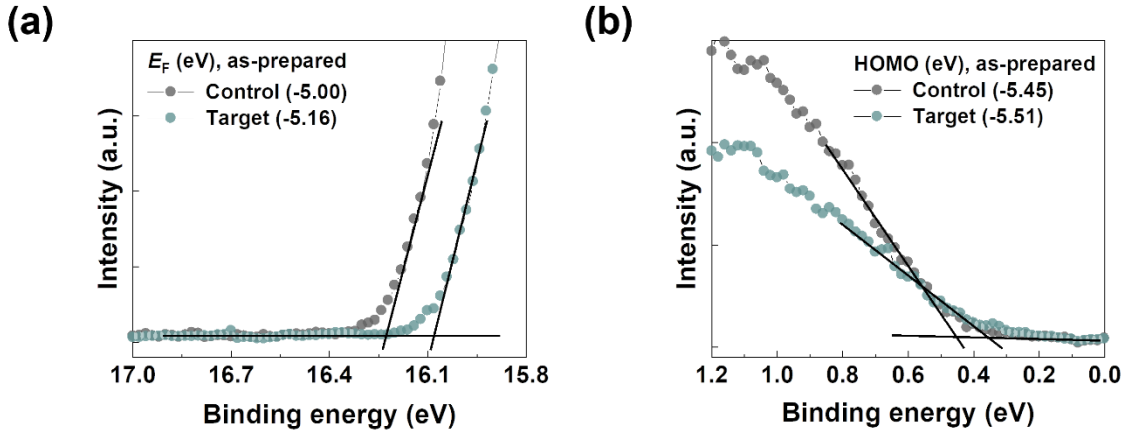

Fig. S10 UPS spectra of the as-prepared spiro-OMeTAD under the control and target conditions; (a) secondary edge region and (b) valence band edge plotted relative to a gold reference.

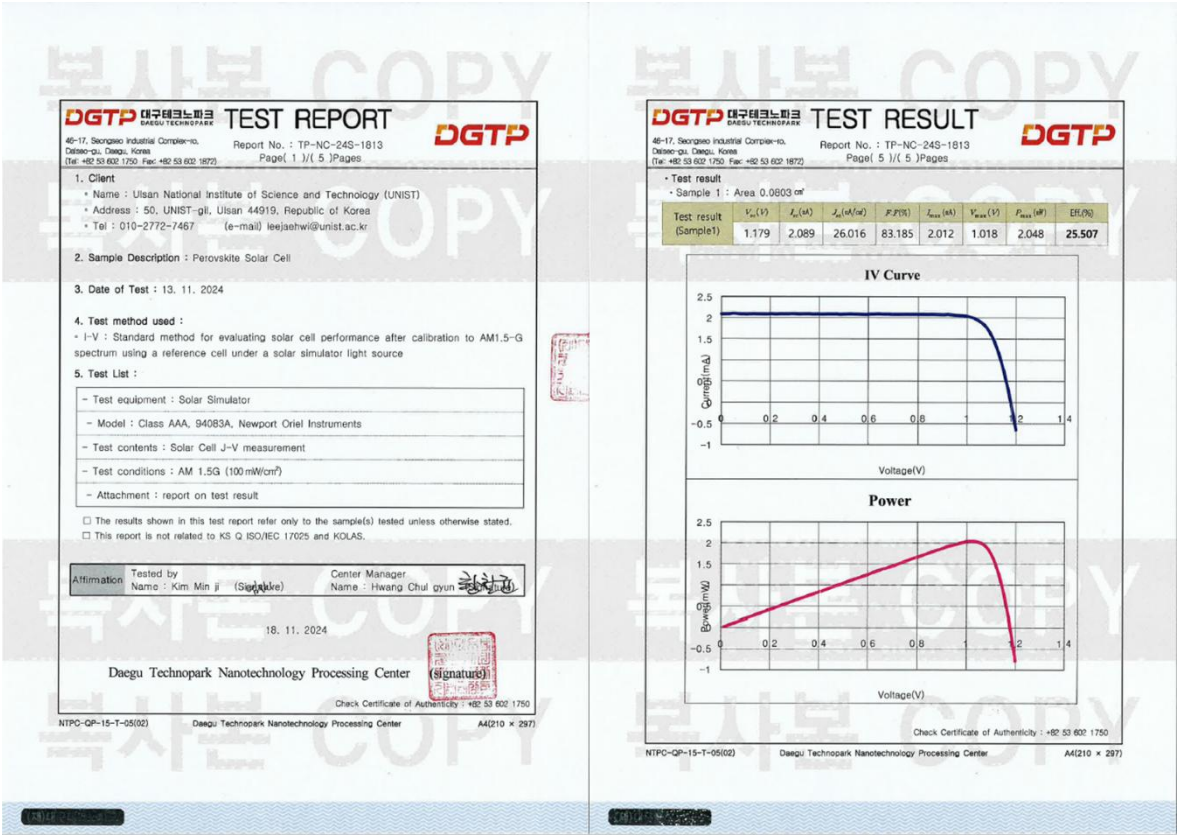

DGTP 대구테크노파크 DAEGU TECHNOPARK TEST REPORT DGTP

46-17, Seongseo Industrial Complex-ro, Dalseo-gu, Daegu, Korea (Tel: +82 53 602 1750 Fax: +82 53 602 1872)

Report No. : TP-NC-24S-1813
Page(1)/(5)Pages

1. Client
- Name : Ulsan National Institute of Science and Technology (UNIST)
- Address : 50, UNIST-gil, Ulsan 44919, Republic of Korea
- Tel : 010-2772-7467 (e-mail) leejaehwi@unist.ac.kr

2. Sample Description : Perovskite Solar Cell

3. Date of Test : 13. 11. 2024

4. Test method used :
- I-V : Standard method for evaluating solar cell performance after calibration to AM1.5-G spectrum using a reference cell under a solar simulator light source

5. Test List :
- Test equipment : Solar Simulator
- Model : Class AAA, 94083A, Newport Oriel Instruments
- Test contents : Solar Cell J-V measurement
- Test conditions : AM 1.5G (100 mW/cm²)
- Attachment : report on test result

☐ The results shown in this test report refer only to the sample(s) tested unless otherwise stated.
☐ This report is not related to KS Q ISO/IEC 17025 and KOLAS.

Affirmation: Tested by Name : Kim Min ji (Signature) Center Manager Name : Hwang Chul gyun

18. 11. 2024

Daegu Technopark Nanotechnology Processing Center (signature)

Check Certificate of Authenticity : +82 53 602 1750

NTPC-QP-15-T-05(02) Daegu Technopark Nanotechnology Processing Center A4(210 × 297)

DGTP 대구테크노파크 DAEGU TECHNOPARK TEST RESULT DGTP

46-17, Seongseo Industrial Complex-ro, Dalseo-gu, Daegu, Korea (Tel: +82 53 602 1750 Fax: +82 53 602 1872)

Report No. : TP-NC-24S-1813
Page(5)/(5)Pages

- Test result
- Sample 1 : Area 0.0803 cm²

Test result (Sample1)	V_{oc}(V)	J_{sc}(mA)	J_{sc}(mA/cm²)	F.F(%)	I_{max}(mA)	V_{max}(V)	P_{max}(mW)	Eff.(%)
	1.179	2.089	26.016	83.185	2.012	1.018	2.048	25.507

Check Certificate of Authenticity : +82 53 602 1750

NTPC-QP-15-T-05(02) Daegu Technopark Nanotechnology Processing Center A4(210 × 297)

Fig. S11 PV performance measured by a photovoltaic certification laboratory (Daegu Techpark, Republic of Korea). The certified efficiency is 25.51%. Standard reporting condition: AM 1.5G 1000.0 W/m^2 at 25.0 °C / scan rate (100 mV/s) / voltage range (1.3 V to -0.05 V) / number of points (100 steps) / aperture area (non-reflective mask with an area of 0.0803 cm^2) / connection (4-wire, rear terminal). Solar simulator: Class AAA, Model 94083A, Serial#: 177 / Lamp model (62726, Serial#: ZGA213P).

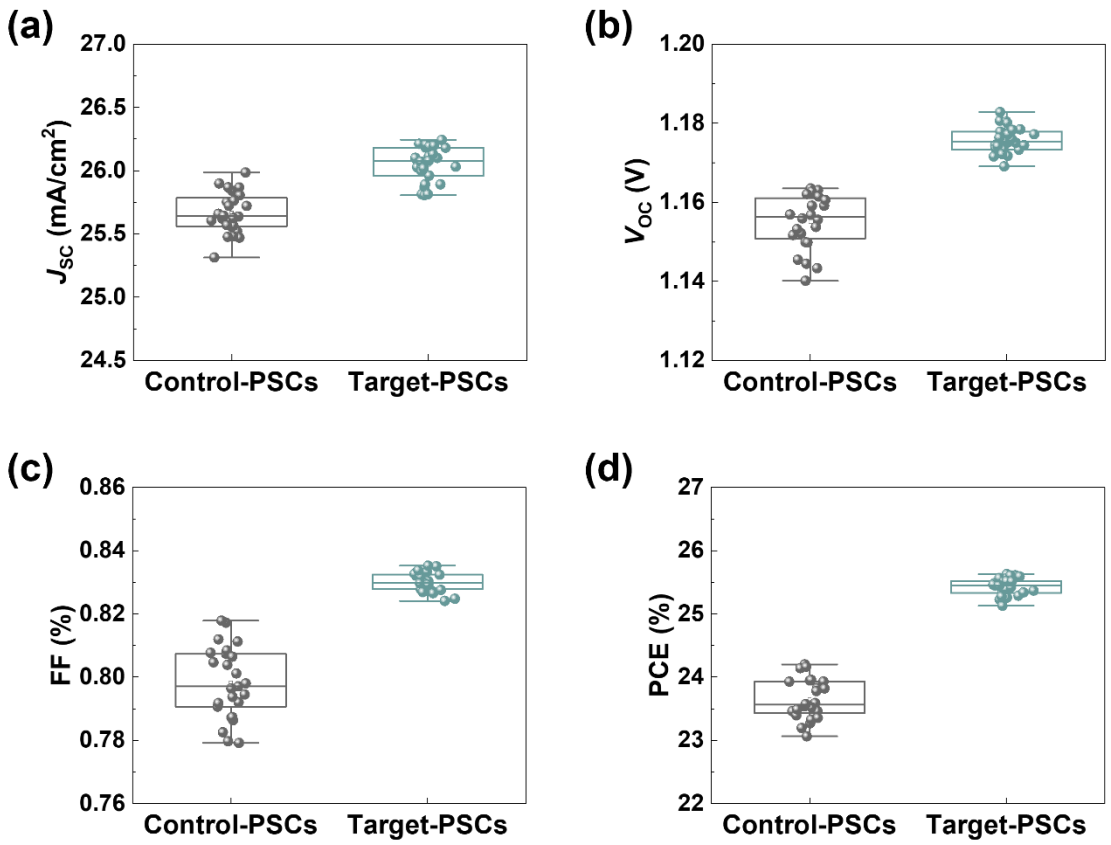

Fig. S12 Statistics of the (a) J_{SC}, (b) V_{OC}, (c) FF, and (d) PCE of the PSCs with the control and target conditions.

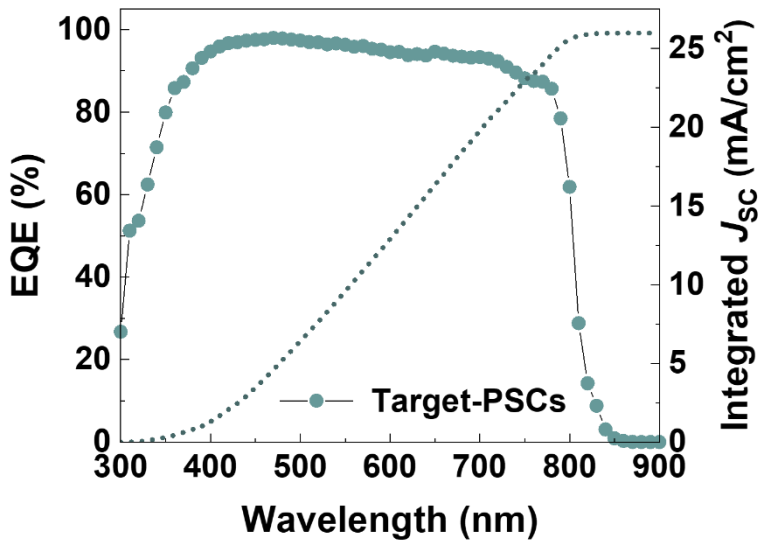

Fig. S13 EQE and the integrated J_{SC} for the PSCs with the target conditions (25.97 mA/cm^2).

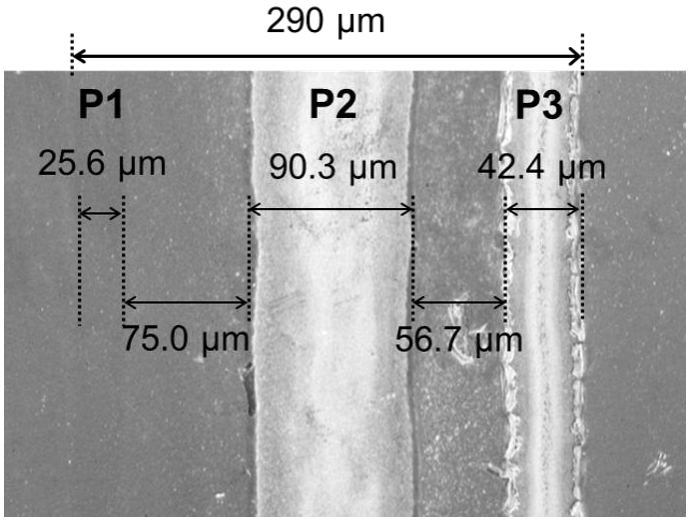

Fig. S14 Photograph showing the separation of sub-cells in the PSMs and related widths for P1, P2, and P3 lines. The GFF can be calculated by the ratio of active area to aperture area and determined to be 94.60% and 86.40% for the PSMs with aperture areas of 25 and 100 cm^2, respectively.

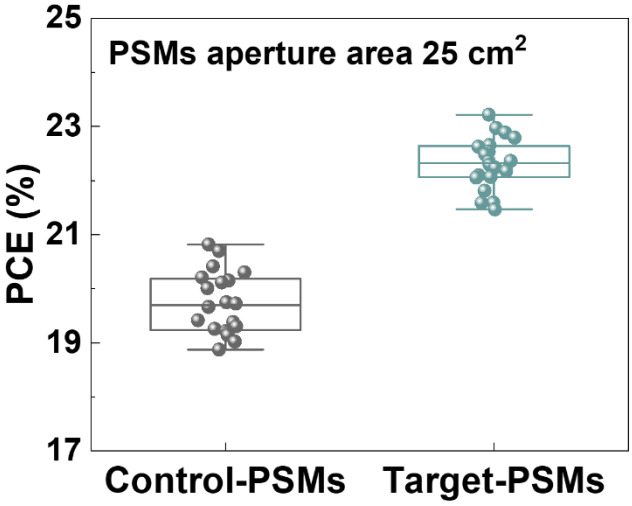

Fig. S15 Statistics of the PCE of the PSMs with an aperture area of 25 cm^2, under the control and target conditions.

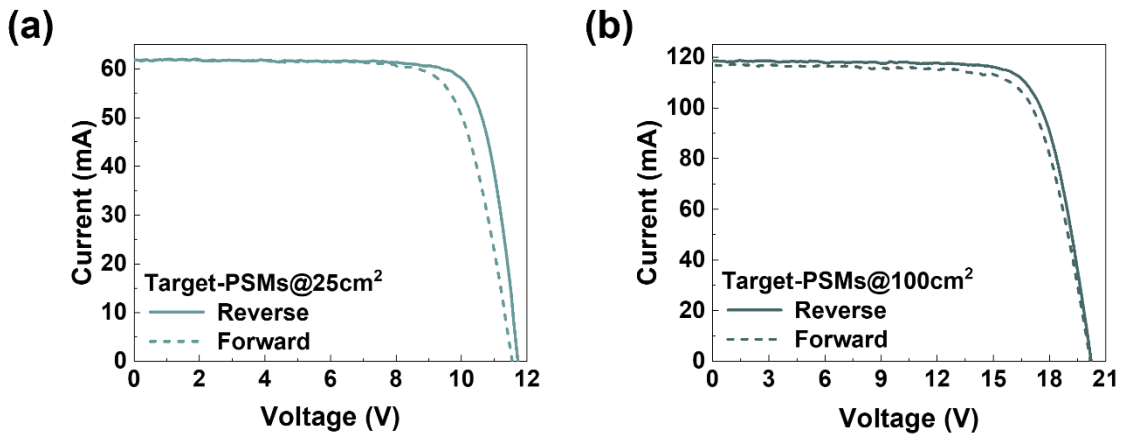

Fig. S16 *I-V* curves of the target-PSMs with aperture areas of (a) 25 and (b) 100 cm^2 under both reverse and forward scanning directions.

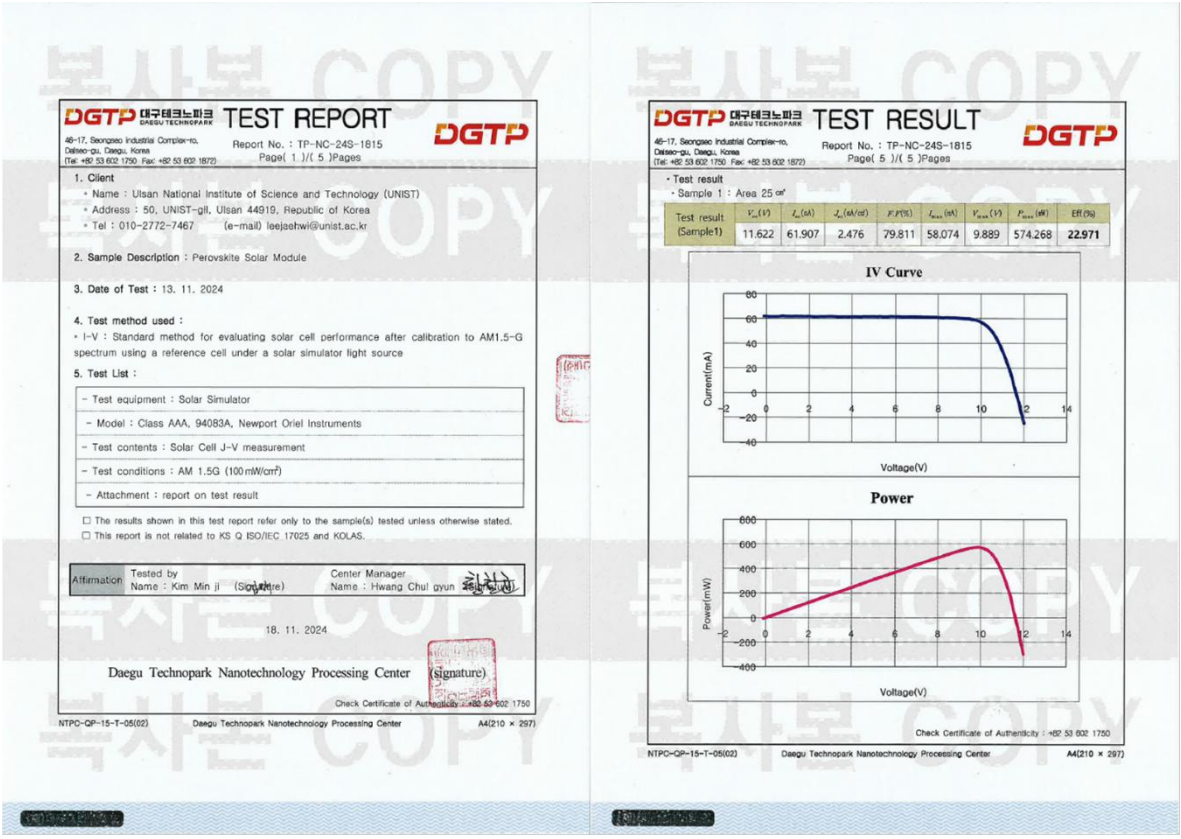

DGTP 대구테크노파크 DAEGU TECHNOPARK TEST REPORT

46-17, Seongseo Industrial Complex-ro, Dalseo-gu, Daegu, Korea (Tel: +82 53 602 1750 Fax: +82 53 602 1872)

Report No. : TP-NC-24S-1815
Page(1)/(5)Pages

1. Client
- Name : Ulsan National Institute of Science and Technology (UNIST)
- Address : 50, UNIST-gil, Ulsan 44919, Republic of Korea
- Tel : 010-2772-7467 (e-mail) leejaehwi@unist.ac.kr

2. Sample Description : Perovskite Solar Module

3. Date of Test : 13. 11. 2024

4. Test method used :
- I-V : Standard method for evaluating solar cell performance after calibration to AM1.5-G spectrum using a reference cell under a solar simulator light source

5. Test List :

- Test equipment : Solar Simulator
- Model : Class AAA, 94083A, Newport Oriel Instruments
- Test contents : Solar Cell J-V measurement
- Test conditions : AM 1.5G (100 mW/cm²)
- Attachment : report on test result

☐ The results shown in this test report refer only to the sample(s) tested unless otherwise stated.
☐ This report is not related to KS Q ISO/IEC 17025 and KOLAS.

Affirmation	Tested by Name : Kim Min ji (Signature)	Center Manager Name : Hwang Chul gyun (Signature)

18. 11. 2024

Daegu Technopark Nanotechnology Processing Center (signature)

Check Certificate of Authenticity : +82 53 602 1750

NTPC-QP-15-T-05(02) Daegu Technopark Nanotechnology Processing Center A4(210 × 297)

DGTP 대구테크노파크 DAEGU TECHNOPARK TEST RESULT

46-17, Seongseo Industrial Complex-ro, Dalseo-gu, Daegu, Korea (Tel: +82 53 602 1750 Fax: +82 53 602 1872)

Report No. : TP-NC-24S-1815
Page(5)/(5)Pages

- Test result
- Sample 1 : Area 25 cm²

Test result	V_{oc} (V)	I_{sc} (mA)	J_{sc} (mA/cm²)	F.F(%)	I_{max} (mA)	V_{max} (V)	P_{max} (mW)	Eff.(%)
(Sample1)	11.622	61.907	2.476	79.811	58.074	9.889	574.268	22.971

Check Certificate of Authenticity : +82 53 602 1750

NTPC-QP-15-T-05(02) Daegu Technopark Nanotechnology Processing Center A4(210 × 297)

Fig. S17 PV performance measured by a photovoltaic certification laboratory (Daegu Techpark, Republic of Korea). The certified efficiency is 22.97%. Standard reporting condition: AM 1.5G 1000.0 W/m^2 at 25.0 °C / scan rate (100 mV/s) / voltage range (12 V to -0.1 V) / number of points (150 steps) / connection (2-wire, rear terminal). Solar simulator: Class AAA, Model 94083A, Serial#: 177 / Lamp model (62726, Serial#: ZGA213P).

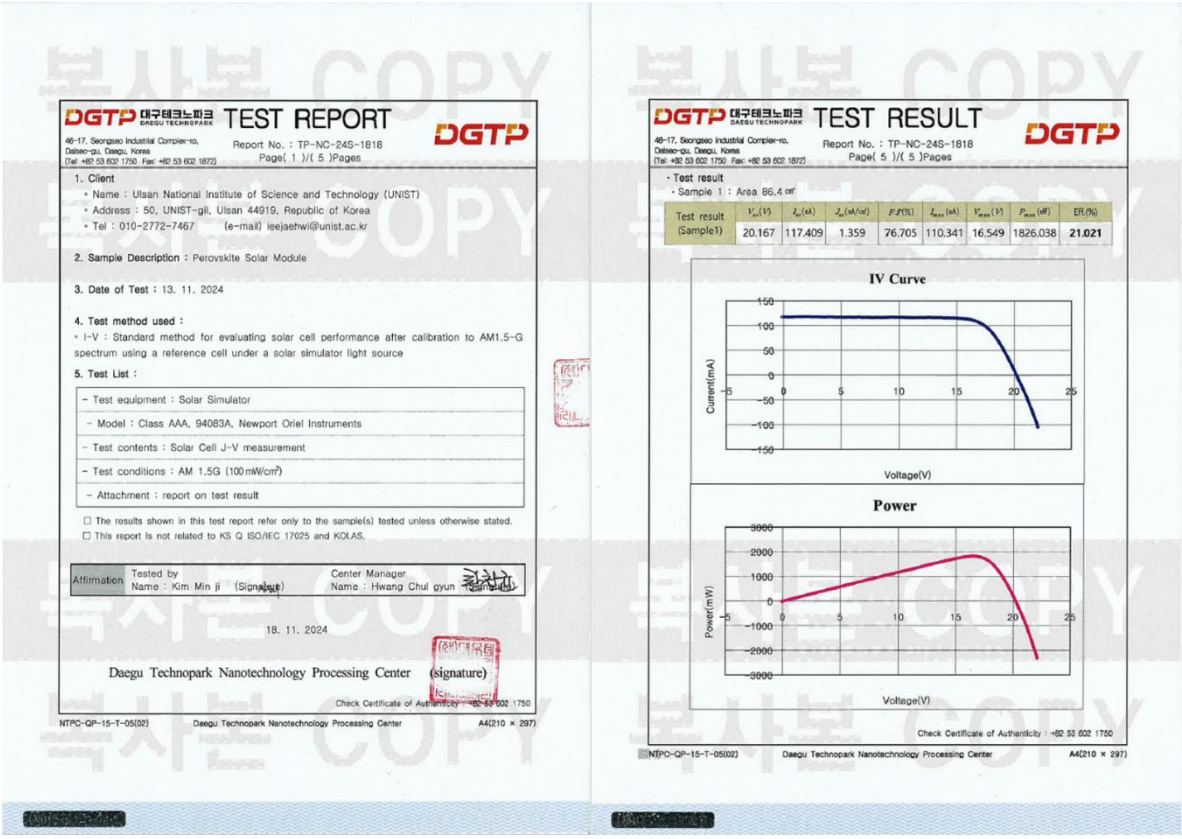

DGTP 대구테크노파크 DAEGU TECHNOPARK TEST REPORT

46-17, Seongseo Industrial Complex-ro, Dalseo-gu, Daegu, Korea (Tel: +82 53 602 1750 Fax: +82 53 602 1872)

Report No. : TP-NC-24S-1818
Page(1)/(5)Pages

1. Client
- Name : Ulsan National Institute of Science and Technology (UNIST)
- Address : 50, UNIST-gil, Ulsan 44919, Republic of Korea
- Tel : 010-2772-7467 (e-mail) leejaehwi@unist.ac.kr

2. Sample Description : Perovskite Solar Module

3. Date of Test : 13. 11. 2024

4. Test method used :
- I-V : Standard method for evaluating solar cell performance after calibration to AM1.5-G spectrum using a reference cell under a solar simulator light source

5. Test List :
- Test equipment : Solar Simulator
- Model : Class AAA, 94083A, Newport Oriel Instruments
- Test contents : Solar Cell J-V measurement
- Test conditions : AM 1.5G (100 mW/cm²)
- Attachment : report on test result

☐ The results shown in this test report refer only to the sample(s) tested unless otherwise stated.
☐ This report is not related to KS Q ISO/IEC 17025 and KOLAS.

Affirmation: Tested by Name : Kim Min ji (Signature) Center Manager Name : Hwang Chul gyun

18. 11. 2024

Daegu Technopark Nanotechnology Processing Center (signature)

Check Certificate of Authenticity : +82 53 602 1750

NTPC-QP-15-T-05(02) Daegu Technopark Nanotechnology Processing Center A4(210 × 297)

DGTP 대구테크노파크 DAEGU TECHNOPARK TEST RESULT

46-17, Seongseo Industrial Complex-ro, Dalseo-gu, Daegu, Korea (Tel: +82 53 602 1750 Fax: +82 53 602 1872)

Report No. : TP-NC-24S-1818
Page(5)/(5)Pages

- Test result
- Sample 1 : Area 86.4 ㎠

Test result (Sample1)	V_{oc}(V)	J_{sc}(mA)	J_{sc}(mA/㎠)	F.F(%)	I_{max}(mA)	V_{max}(V)	P_{max}(mW)	Eff.(%)
	20.167	117.409	1.359	76.705	110.341	16.549	1826.038	**21.021**

Check Certificate of Authenticity : +82 53 602 1750

NTPC-QP-15-T-05(02) Daegu Technopark Nanotechnology Processing Center A4(210 × 297)

Fig. S18 PV performance measured by a photovoltaic certification laboratory (Daegu Techpark, Republic of Korea). The certified efficiency is 21.02%. Standard reporting condition: AM 1.5G 1000.0 W/m^2 at 25.0 °C / scan rate (100 mV/s) / voltage range (25 V to -0.1 V) / number of points (200 steps) / connection (2-wire, rear terminal). Solar simulator: Class AAA, Model 94083A, Serial#: 177 / Lamp model (62726, Serial#: ZGA213P).

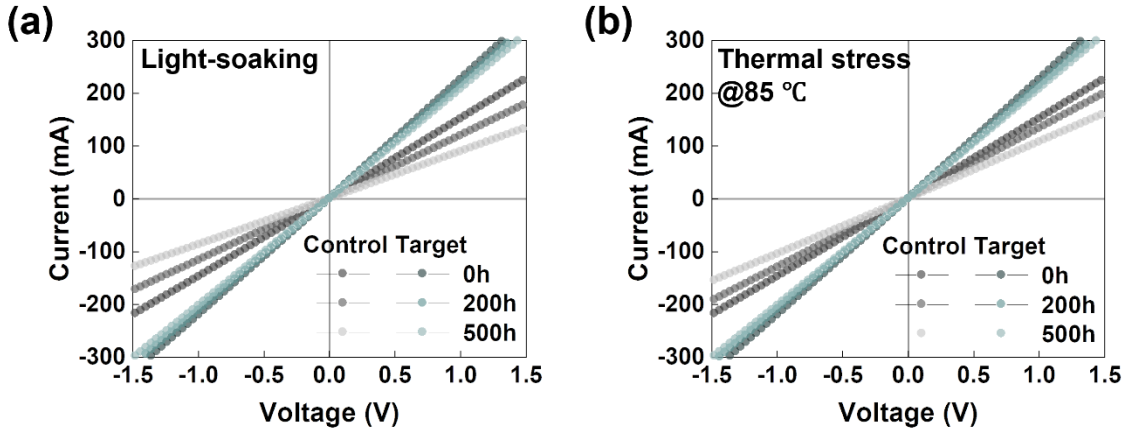

Fig. S19 Variation of *J-V* curves measured with device of FTO/spiro-OMeTAD/Au under (a) light illumination and (b) thermal stress at 85 ℃, respectively.

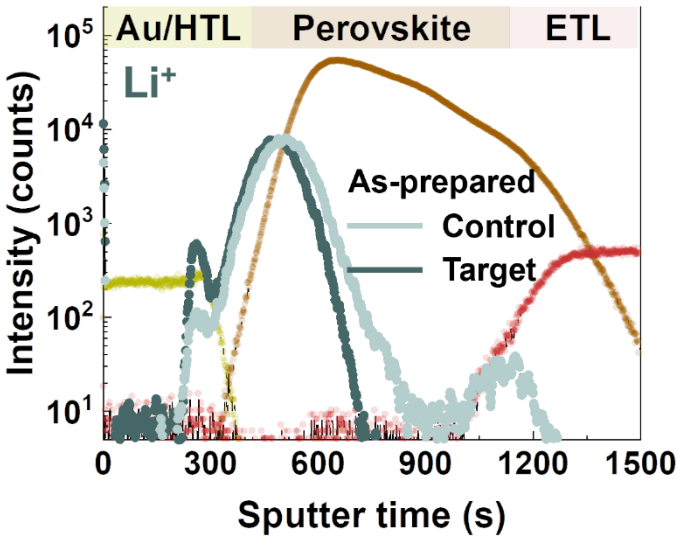

Fig. S20 ToF-SIMS depth profiles of Li^+ ions in device of FTO/SnO_2/perovskite/spiro-OMeTAD/Au, before being subjected to light illumination and thermal stress at 85 ℃.

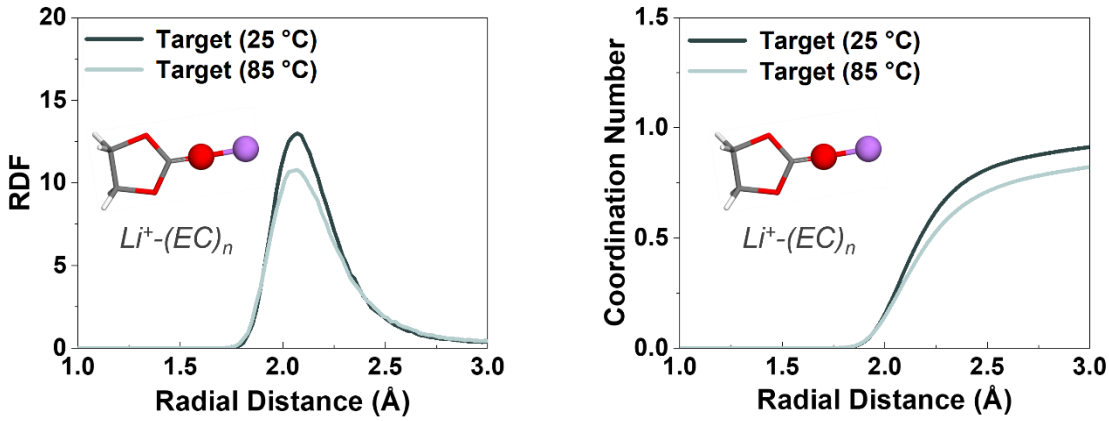

Fig. S21 Radial distribution function (left) and coordination number (right) of the Li^+ ion with EC under different temperature conditions (*i.e.*, 25 ℃ and 85 ℃).

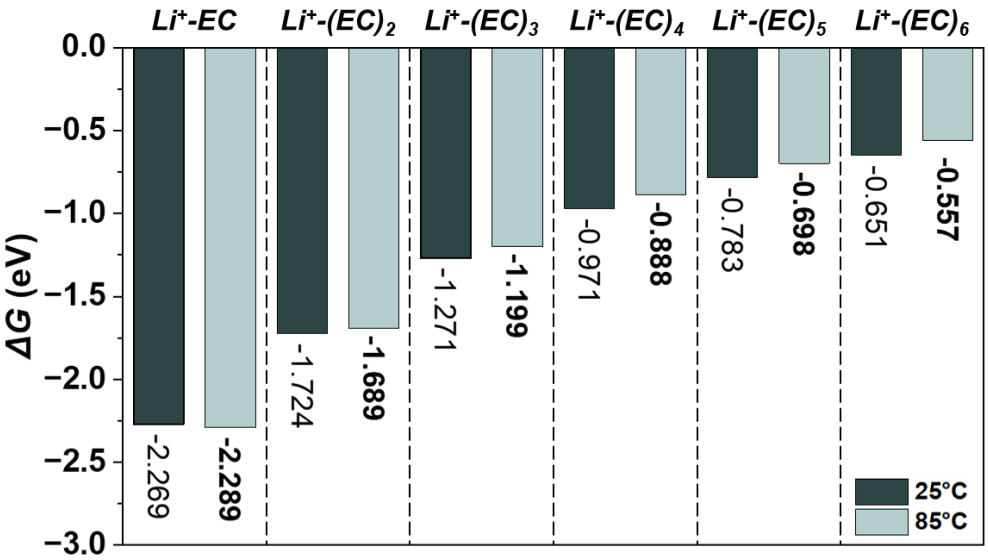

Fig. S22 Binding Gibbs free energies (ΔG) of the Li^+ ion with $(EC)_n$ under different temperature conditions (*i.e.*, 25 ℃ and 85 ℃).

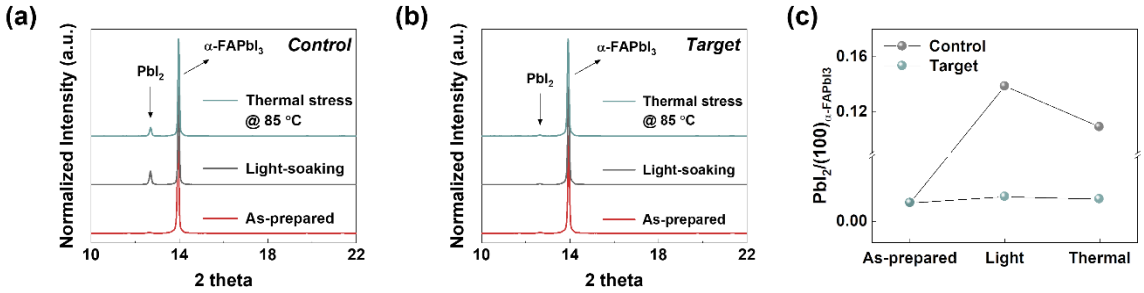

Fig. S23 XRD patterns of perovskite films. The perovskite films were coated once with spiro-OMeTAD under the control and target conditions, followed by the deposition of a gold electrode. Samples were exposed to (a) light illumination and (b) thermal stress at 85 ℃, respectively. To investigate XRD patterns of the perovskite films, spiro-OMeTAD films were removed by washing with chlorobenzene. (c) The ratio of intensity for PbI_2 peak to that for (001) $FAPbI_3$ peak.

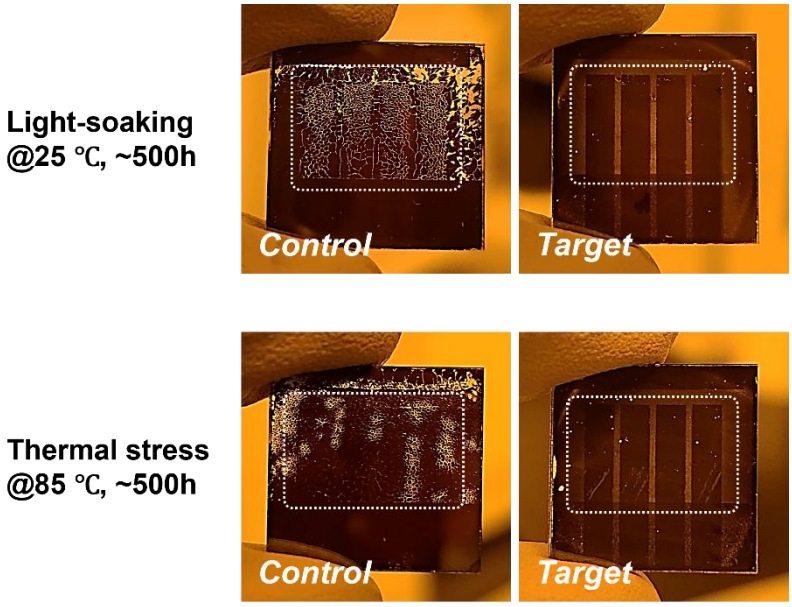

Fig. S24 Photographs showing the perovskite films. The perovskite films were coated once with spiro-OMeTAD under the control and target conditions, followed by the deposition of a gold electrode. Samples were exposed to light illumination and thermal stress at 85 ℃, respectively. After then, spiro-OMeTAD films were removed by washing with CB.

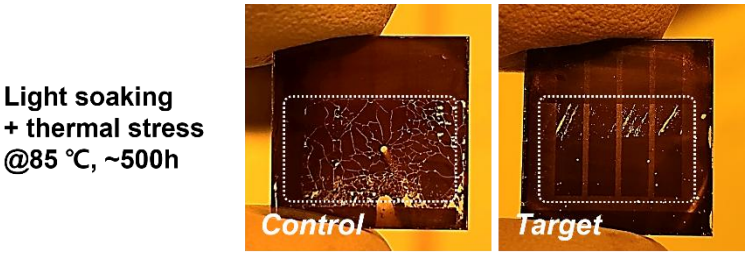

Fig. S25 Photographs showing the perovskite films. The perovskite films were coated once with spiro-OMeTAD under the control and target conditions, followed by the deposition of a gold electrode. Samples were exposed to simultaneous light illumination and thermal stress at 85 ℃. After then, spiro-OMeTAD films were removed by washing with CB.

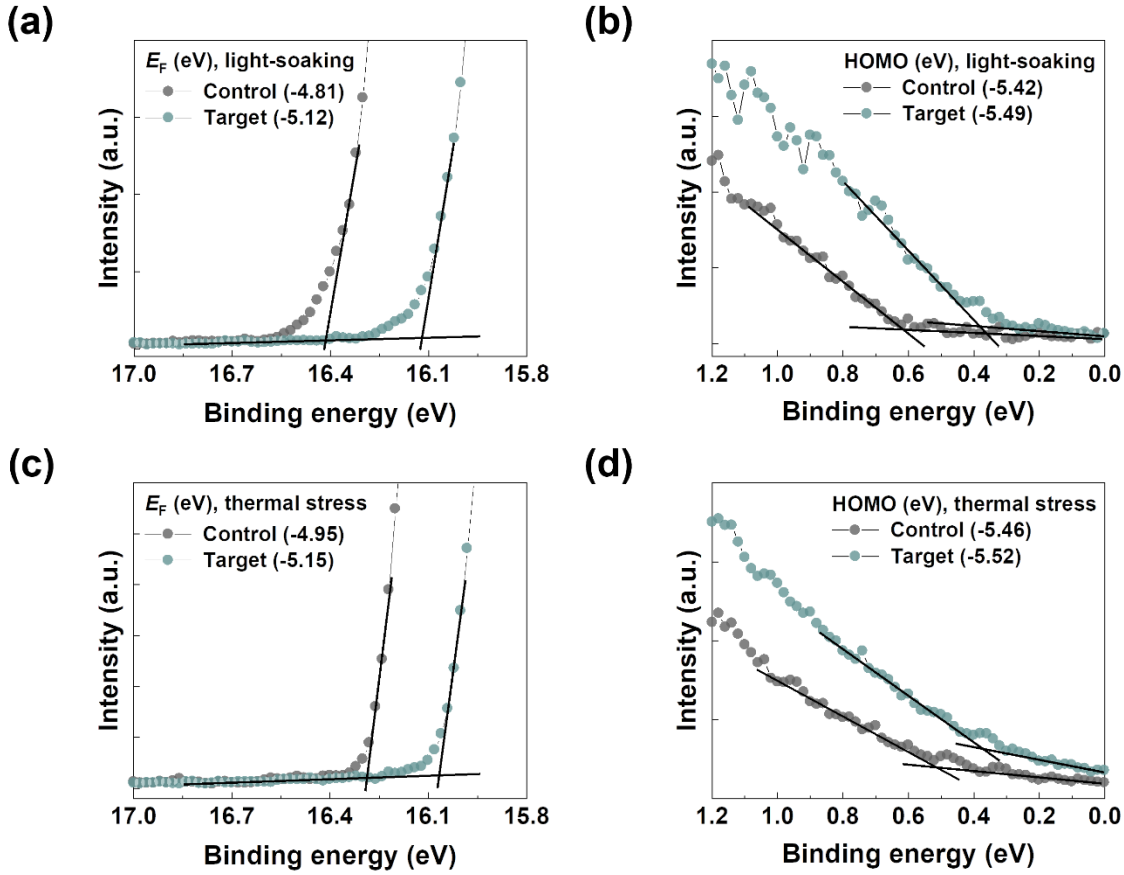

Fig. S26 UPS spectra of the spiro-OMeTAD under the control and target conditions; (a, c) secondary edge region and (b, d) valence band edge plotted relative to a gold reference. Samples were exposed to light illumination and thermal stress at 85 °C, respectively.

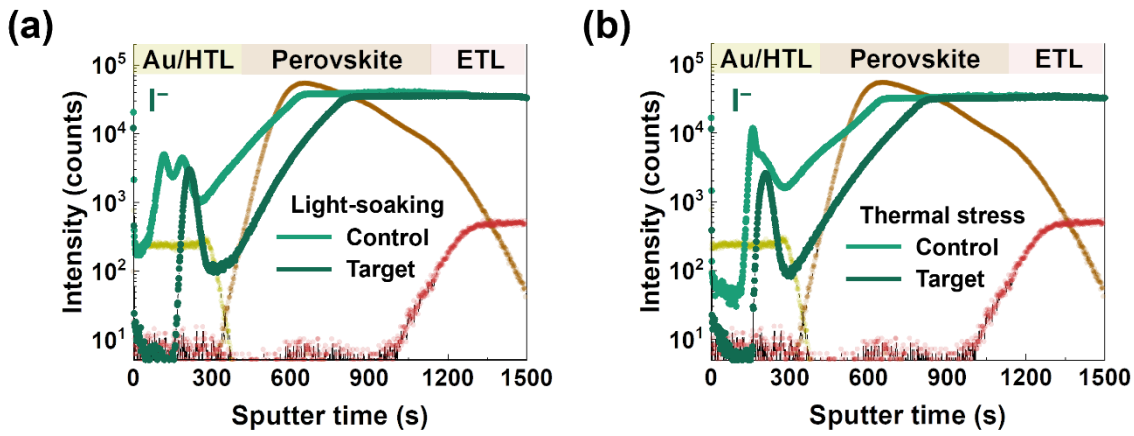

Fig. S27 ToF-SIMS depth profiles of I^- ions in device of FTO/SnO_2/perovskite/spiro-OMeTAD/Au, after being subjected to (a) light illumination and (b) thermal stress at 85 °C for 500 hours.

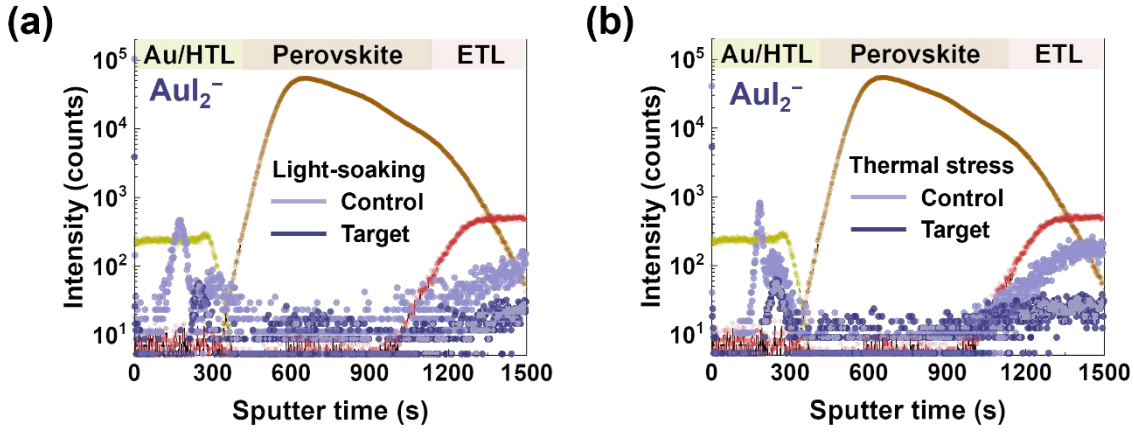

Fig. S28 ToF-SIMS depth profiles of AuI_2^- ions in device of FTO/SnO_2/perovskite/spiro-OMeTAD/Au, after being subjected to (a) light illumination and (b) thermal stress at 85 °C for 500 hours.

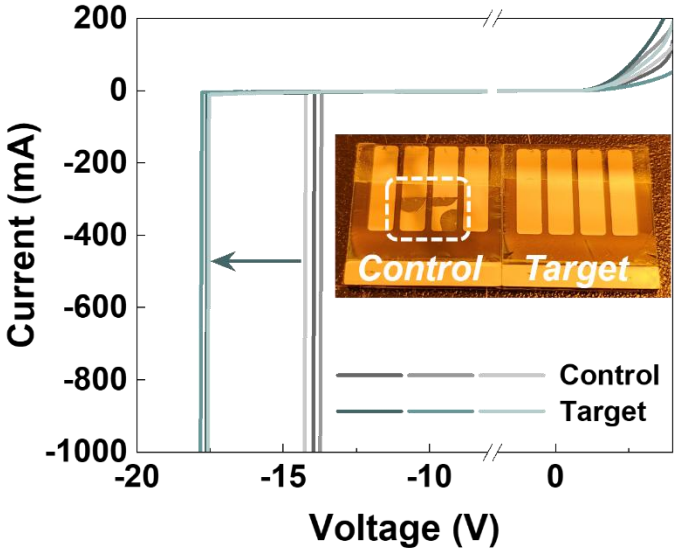

Fig. S29 *J-V* curves of control and target PSCs measured from 4 V to -20 V to determine the breakdown voltage.

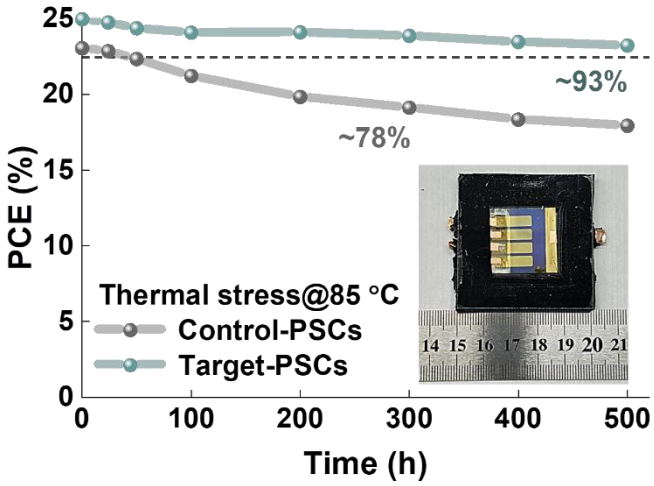

Fig. S30 Thermal stability of the encapsulated PSCs subjected to thermal stress at 85 ℃ (15% RH).

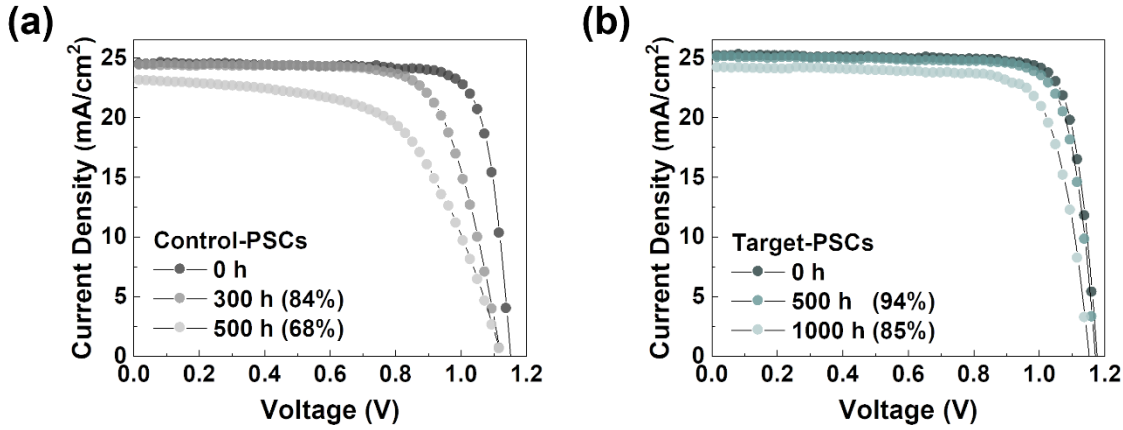

Fig. S31 Variation of *J-V* curves of the (a) control- and (b) target-PSCs under the damp-heat (85 °C/85% RH) conditions.

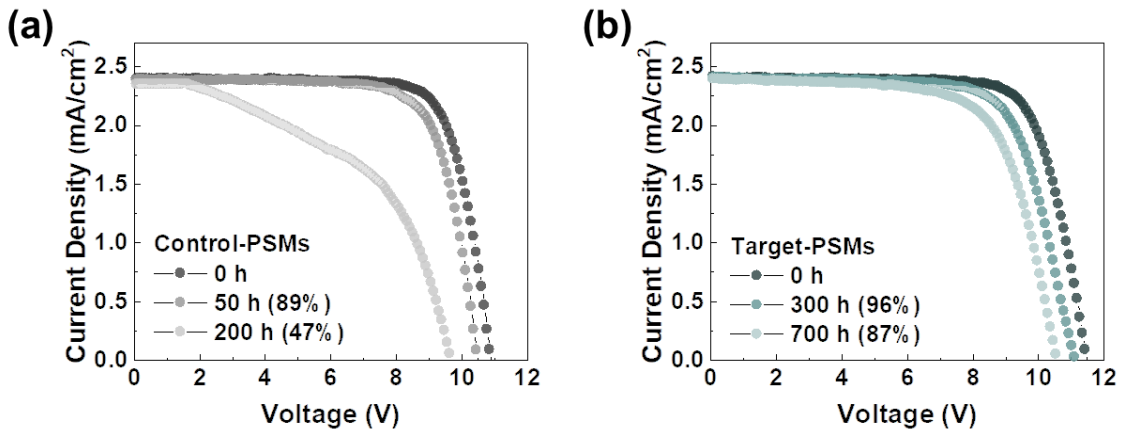

Fig. S32 Variation of *J-V* curves of the (a) control- and (b) target-PSMs with an aperture area of 25 cm^2 under the damp-heat (85 °C/85% RH) conditions.

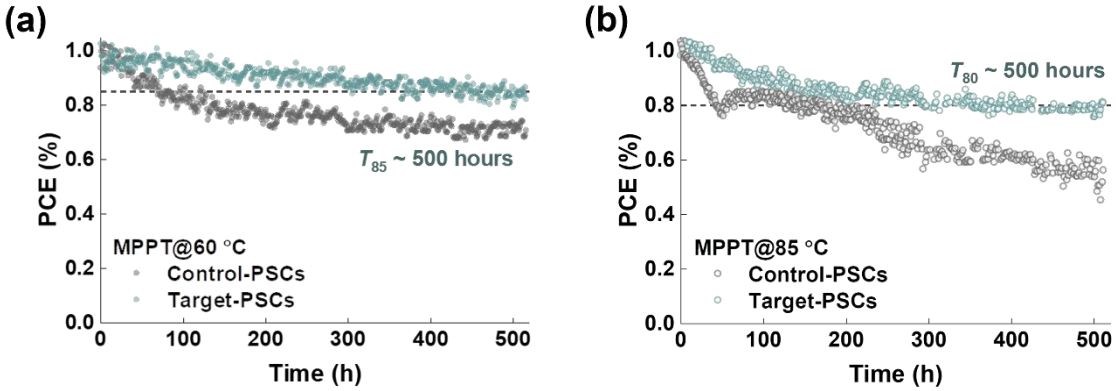

Fig. S33 MPPT of the encapsulated PSCs at (a) 60 ℃ and (b) 85 ℃ under 1-sun illumination.

Table S1. Number of molecules in model systems for molecular dynamics simulations.

Model system	Li^+ ion	$TFSI^-$ ion	EC
Control	1200	1200	0
Target	700	700	700

Table S2. Detailed *J-V* parameters of the PSCs using spiro-OMeTAD under the control and target conditions.

	V_{OC} (V)	J_{SC} (mA/cm^2)	FF (%)	PCE (%)
Control-PSCs	1.162	25.868	80.38	24.16
Target-PSCs	1.180	26.031	83.18	25.56

Table S3. Detailed *J-V* parameters and materials of previously reported PSCs using *t*BP-free spiro-OMeTAD HTLs.

Published year	Materials	Photovoltaic parameters				Module	Ref.
		V_{OC} (V)	J_{SC} (mA/cm^2)	FF (%)	PCE (%)		
2017.06	TBA-TFSI	1.071	22.3	77	18.4	-	*ACS Energy Lett.* **3**, 1677-1682 (2018)
2017.08	$Mo(tfd\text{-}COCF_3)_3$	1.07	22.11	76	17.8	-	*ACS Energy Lett.* **2**, 2044-2050 (2017)
2018.09	BMPy-TFSI	1.020	21.17	65.12	14.06	-	*Joule* **2**, 1800-1815 (2018)
2018.09	$Cu(dpm)_2(PF_6)_2$	1.12	22.8	75	19.3	-	*ACS Nano* **12**, 10452-10462 (2018)
2020.05	TPFB	1.141	23.44	75.29	20.10	-	*ACS Appl. Mater. Interfaces* **12**, 23874-23884 (2020)
2020.06	PFPPY	1.12	23.98	79.62	21.38	-	*Nano Energy* **72**, 104673 (2020)
2021.09	Sb_2S_3	1.132	24.75	79	22.13	-	*Sol. RRL* **5**, 2100622 (2021)
2022.06	POM@MOF	1.11	24.1	80.0	21.5	-	*Nano Energy* **97**, 107184 (2022)
2022.07	DIC-PBA	1.14	24.29	82.1	22.73	-	*Joule* **6**, 1689-1709 (2022)
2022.07	TBMP-TFSI & Spiro-$OMeTAD(TFSI)_2$	1.175	25.52	83.88	25.15	-	*Science* **377**, 495-501 (2022)
2024.01	IP-TFSI	1.19	25.07	84.35	25.16	20.71% (15.03 cm^2)	*Angew. Chem. Int. Ed.* **63**, e202316183 (2024)
2024.06	Spiro-$OMeTAD(TFSI)_x$	1.156	25.59	81.7	24.18	-	*Adv. Energy Mater.* **14**, 2400456 (2024)
	Ethylene carbonate	**1.180**	**26.031**	**83.18**	**25.56**	**23.22 (25 cm^2) 22.14% (100 cm^2)**	**This work**

Table S4. Detailed *J-V* parameters of the PSMs with an aperture area of 25 cm^2 using spiro-OMeTAD under the control and target conditions.

25 cm^2	V_{OC} **(V)**	I_{SC} **(mA)**	J_{SC} **(mA/cm^2)**	**FF (%)**	**PCE (%)**
Control-PSCs	11.36	60.98	2.439	74.37	20.60
Target-PSCs	11.72	61.87	2.475	80.04	23.22

Table S5. Detailed *J-V* parameters of the PSMs with an aperture area of 100 cm^2 using spiro-OMeTAD under the control and target conditions.

100 cm^2	V_{OC} **(V)**	I_{SC} **(mA)**	J_{SC} **(mA/cm^2)**	**FF (%)**	**PCE (%)**
Control-PSCs	19.19	116.7	1.351	76.61	19.86
Target-PSCs	20.22	118.6	1.373	79.74	22.14

Table S6. Detailed *J-V* parameters of the PSMs with the target conditions under both reverse and forward scanning directions.

Target-PSMs	Scan direction	V_{OC} (V)	I_{SC} (mA)	J_{SC} (mA/cm^2)	FF (%)	PCE (%)	Hysteresis index
25 cm^2	Reverse	11.72	61.87	2.475	80.04	23.22	0.073
	Forward	11.55	61.75	2.470	75.44	21.52	
100 cm^2	Reverse	20.22	118.6	1.373	79.74	22.14	0.081
	Forward	20.18	117.0	1.354	74.45	20.34	

Supplementary References

S1 B. Delley. *J. Chem. Phys.*, 1990, **92**, 508-517.

S2 B. Delley. *J. Chem. Phys*., 2000, **113**, 7756-7764.

S3 A. D. Becke. *J. Chem. Phys.*, 1993, **98**, 5648-5652.

S4 P. J. Stephens, F. J. Devlin, C. F. Chabalowski and M. J. Frisch. *J. Phys. Chem.*, 1994, **98**, 11623-11627.

S5 A. Tkatchenko and M. Scheffler, *Phys. Rev. Lett.*, 2009, **102**, 073005.

S6 R. L. C. Akkermans, N. A. Spenley and S. H. Robertson, *Mol. Simul.*, 2021, **47**, 540-551.

S7 I. Leontyev and A. Stuchebrukhov, *Phys. Chem. Chem. Phys.*, 2011, **13**, 2613-2626.

S8 C. Park, M. Kanduč, R. Chudoba, A. Ronneburg, S. Risse, M. Ballauff and J. Dzubiella. *J. Power Sources*, 2018, **373**, 70-78.

S9 H. J. C. Berendsen, J. P. M. Postma, W. F. van Gunsteren, A. DiNola and J. R. Haak, *J. Chem. Phys.*, 1984, **81**, 3684-3690.